Simulation of energy harvesting from roads via pyroelectricity

Ashok K. Batra
Sudip Bhattacharjee
Ashwith Kumar Chilvery
Mohan D. Aggarwal
Matthew E. Edwards
Amar Bhalla

Simulation of energy harvesting from roads via pyroelectricity

Ashok K. Batra,[a] Sudip Bhattacharjee,[b] Ashwith Kumar Chilvery,[a]
Mohan D. Aggarwal,[a] Matthew E. Edwards,[a] and Amar Bhalla[c]
[a] Alabama A&M University, Department of Physics (Materials Science Group),
Normal, Alabama 35762
ashok.batra@aamu.edu
[b] Alabama A&M University, Department of Civil Engineering, Normal, Alabama 35762
[c] University of Texas at San Antonio, Department of Electrical and Computer Engineering,
San Antonia, Texas 79249

Abstract. Power harvesting is the process of extracting useful electrical energy from ambient low grade energy sources such as solar energy, mechanical energy, and thermal energy using smart materials as transducers. These materials have the ability to convert one form of energy into another. This paper aims at thermal-electrical energy converters based on a pyroelectric effect for energy harvesting, and examines its possible use in ultralow power devices and sensor modules. The present work investigates theoretically the energy harvesting capacity of pyroelectric samples fabricated in our laboratory and commercially available pyroelectric elements/transducers by capturing thermal energy of pavements. The single- and polycrystalline elements: triglycine selenate; lithium tantalate; modified lead zirconate titanate; modified lead titanate; modified lead metaniobate; and pyroelectric polymer nanocomposites such as Portland cement; nanocarbon fibers; polymer-lithium tantalate embedded with silver nanoparticles; and others were characterized for applicable performance parameters. The modeling and numerical simulation of energy harvesting capacity of these samples with the available pavement's temperature-profile data over an extended period of time were investigated. The results indicate that the electrical energy harvesting via pyroelectricity is a feasible technique for powering autonomous low-duty electric devices. Based on our analysis of a single electric-energy harvesting unit, the triglycine selenate elements shall perform better than others with regard to the amount of voltage and energy densities extracted with respect to time. Possible future work and concepts of developing promising multidomain energy harvesters or hybrid harvesters are also briefly discussed. © *2011 Society of Photo-Optical Instrumentation Engineers (SPIE)*. [DOI: 10.1117/1.3656395]

Keywords: ambient energy harvesting; dielectric constant; pyroelectric coefficient; pavement; energy capacity; modeling and simulation.

Paper 11180RR received Feb. 3, 2011; revised manuscript received Aug. 12, 2011; accepted for publication Oct. 5, 2011; published online Oct. 31, 2011.

1 Introduction

Energy harvesting or energy scavenging technology allows capturing unused ambient energy such as vibration, strain, light, temperature gradients and variations, energy of gas and liquid flows, and converting into usable electrical energy. Due to advances in low-power portable microelectronics, the batteries in general provide a finite amount of power. Energy harvesting is a perfect match for these as well as wireless devices which otherwise depend on battery power. Thus, it can provide sustained, cost-effective, and environment friendlier solutions for various low-power applications. In the recent past, to provide sustained power to these micro- and nan-

odevices, these unconventional methods for waste energy harvesting and scavenging are being explored.[1–3] Efforts have been made to recover electric power from mechanical vibrations,[1,2] light,[3] and spatial and temporal temperature variations.[3] Waste thermal and mechanical energy of asphalts' pavement can also be a potential source for low-power electronics; to date, this concept has not been explored in particular via pyroelectricity. However, recently efforts are being made in large scale in Israel by paving kilometers of roads with a specially designed series of piezoelectric modules.[4,5]

The amazing pyroelectric materials basically convert most of the electromagnetic radiations spectrum (ultraviolet, infrared, microwave, x-rays, terahertz) energy into electrical energy, mean transforms photons to phonons to electrons.[6] Thus, these materials can be exploited to convert thermal energy into electricity. The pyroelectrics are mainly used as uncooled wide-band infrared detectors included in numerous scientific and medical instruments.[6] A popular application of the pyroelectric element is in the regular household motion burglar's alarm/sensors. The slight change in temperature from infrared radiations emitted by human bodies in motion, produces electric charges on the surface of the pyroelectric sensor's element, and hence triggers an alarm. In particular, a charge is produced when the material's temperature is altered (increase or decrease) as a function of time by any suitable means. In the recent past, researchers have started exploring the pyroelectrics and piezoelectrics as possible energy harvesters on both theoretical and experimental arenas.[1–3,7–10] Most of the innovative research deals with harvesting from vibrations[8] and a very few deal with harvesting via pyroelectricity.[11–15] The performance of pyroelectric materials depends strongly on their thermophysical and electrical properties. There are only a few high performance pyroelectrics known so far suitable for infrared detecting and imaging devices, both in single- and polycrystalline and composite forms: triglycine sulfate (TGS) family, lithium tantalate (LT), barium strontium titanate, polyvinylidene fluoride (PVDF) and its co-polymers, modified lead zirconate tantalate (PZT), poly (vinylidene fluoride-trifluoroethylene) [P(VDF-TrFE)]:PZT, and others.[6,16–20] Energy harvesting is generally based on Ericsson pyroelectric cycles in a relaxor ceramic of lead magnesium niobate-lead titanate $[0.9Pb\,(Mg_{0.34}Nb_{0.66})\,O_3\text{-}0.10(PbTiO_3;\ PMN\text{-}PT)]$.[21] Zhu et al. did the simulation for harvested energy based on ferroelectric-paraelectric (FE-PE) transition in $Pb(Zn_{.34}Nb_{.66})0.955Ti_{0.045}O_3$ single crystal which led to 500 mJ/g for an applied field equal to 50 kV/mm.[22] Xie et al. investigated energy harvesting from high temperature increase (45°C to 140°C in ∼10 s: 15°C/s heating rate), i.e., pyroelectric effect using the PZT sample via simple modeling and found that measured and predicted results showed good agreement with peak power density of 0.23 μW/cm^2.[15] It is worth mentioning that such heating rate (15°C/s) sources are generally not available. Navid et al. worked on purified and porous P(VDF-TrFE) in order to improve the figure-of-merit for energy harvesting ($F_E = p^2/\varepsilon'$). For the commercial, purified, and porous films, F_E was 7.93, 10.17, and 5.24 J/m$^3 \cdot$K^2, respectively.[23] The composites, polymer-pyroelectrics, to the best of the authors' knowledge, have not been investigated for energy harvesting applications. Composites contain two or more chemically different materials or phases. The composites show properties derived from individual components.[18,24] The mechanical strength of polymer (PVDF) and high pyroelectric activity (but low strength) of PZT creates high-strength functional PVDF:PZT composites. Thus, it is possible to tailor electrical, pyroelectric, and other physical properties of these materials as per the requirements of the specific application. Several researchers including the authors of this paper have investigated pyroelectric, piezoelectric, and other physical properties of composites.[18,24] Wen and Chung investigated the pyroelectric behavior of cement-based materials.[25] These researchers showed that the steel/carbon-nanofibers increase the dielectric properties of cement composites. Recently, the preliminary investigations by Batra et al. of pyroelectric polymer composites: silver nanoparticles embedded in P(VDF-TrFE):LT, indicate an enhancement in pyroelectric performance as compared with virgin P(VDF-TrFE):LT composites.[26]

Electric energy harvesting, to the best of our knowledge, by application of pyroelectricity via the temporal temperature fluctuations of pavements (thermal energy of roads), has not been investigated. The proposed concept and features, if realized in practice, could ensure sustained

and uninterrupted power supply to wireless microsensors, pavement-management-system hardware, and other civil engineering applications; thereby providing a contribution to energy conservation. Further, electrical and pyroelectric investigations of important pyroelectric materials are warranted with regard to their applications in energy harvesting roads. In the present paper, the electrical and pyroelectric properties of high performance single- and polycrystalline and composite materials including those designed/fabricated by the authors have been investigated. An appropriate model and foregoing parameters were utilized to numerically simulate the voltage and electrical energy generated via the pyroelectric effect, stored in a capacitor over an extended period of time.[14] The available pavement's temperature data in Huntsville, Alabama were incorporated as a heat-energy source. The use of single crystals of the TGS family, triglycine selenate (TGSe), for energy harvesting roads was predicted to be better than other candidate materials. Finally, the potential of harvesting electrical energy from pavement's temperature variation via pyroelectric effect is also discussed including via piezoelectricity as pyroelectric materials are also piezoelectric.

2 Experimental Details and Methodology

2.1 Materials Selected

A brief description of the characteristics of pyroelectric materials is worth presenting for lucidity.

All crystalline materials are categorized into one of the possible 32 different classes, i.e., point groups divided by using the symmetry elements: i. center of symmetry, ii. axes of rotation, iii. mirror planes, and iv. several combinations of them. The 32 point groups are subdivisions of 7 basic crystal systems that are, in order of ascending symmetry, triclinic, monoclinic, orthorhombic, tetragonal, rhombohedral (trigonal), hexagonal, and cubic. Eleven of these forms are centrosymmetric. Of the remaining 21 noncentrosymmetric groups, 20 are piezoelectrics, meaning that these materials produce an electric surface charge in response to applied mechanical stress. Of the 20 piezoelectric crystal classes, 10 crystals have a permanent electric dipole, and equilibrium of the electrostatic potential caused by this dipole is distorted by mechanical stress (piezoelectricity) or temperature change (pyroelectricity). Certain pyroelectrics can be further divided as ferroelectric materials. The ferroelectric group is a subgroup of the spontaneously polarized pyroelectric crystals. On one hand, the polarization of ferroelectric is similar to the polarization of pyroelectric. On the other hand, there is a difference between the two polarizations because the ferroelectric polarization is reversible by an external applied electric field, provided that the applied field is less than the dielectric breakdown of the materials. Therefore, materials that can be defined as ferroelectrics must have two characteristics: 1. the presence of spontaneous polarization and 2. reversibility of the polarization under an electric field. A ferroelectric material is therefore both pyroelectric and piezoelectric, and these materials are also termed as smart materials.[19,23]

The pyroelectric materials and appropriate electrical circuit for ultimately designing a single domain 'micro-electric harvester' for the modeling and numerical simulation for their energy harvesting from pavements via pyroelectricity are presented in Table 1 and Fig. 1, respectively. A variety of materials were selected from three categories: i. single crystalline: TGSe, LT; ii. polycrystalline: lead metaniobate (PN), doped lead lanthanum zirconate titanate, lead lanthanum zirconate titanate (PLZT), modified lead metaniobate (PN), lead lanthanum zirconate titanate (8/40/60; PLZT-1), modified lead titanate (MPT); and iii. polymer pyroelectric composites: Portland cement:nanocarbon fibers and silver nanoparticles embedded in P(VDF-TrFE):LT(PVT:LT-Ag).

a. Single crystalline pyroelectric materials: Triglycine selenate [$(CH_2NH_2COOH)_3$. H_2SeO_4; TGSe], a well-known pyroelectric material with monoclinic crystal structure is used for room-temperature infrared detectors. Its Curie temperature is in the vicinity of 22°C, thus leading to very high pyroelectric activity around ambient temperatures.[19]

Table 1 Properties of investigated smart materials; Pyroelectric coefficient (p, nC/cm^{2}K), dielectric constant (ε'; real part).

No.	Material	Acronym	Sample Form	Pyroelectric Coefficient (P)	Dielectric Constant (ε')	References
1	Doped Lead Lanthanum Zirconate Titanate	DPLZT	Bulk Ceramic	41	768	20
2	Lead Lanthanum Zirconate Titanate	PLZT	Bulk Ceramic	45	700	20
3	PZT Multilayer	PZTML	Thin-Films	34	845	20
4	Triglycine Selenate	TGSe	Bulk Single Crystals	420	420	20
5	Lead Lanthanum Zirconate Titanate (8/40/60)	PLZT-1	Bulk Ceramic	120	429	20
6	Lithium Tantalate	LT	Bulk Single Crystals	f(T)*	f(T)*	Present work
7	PVDF-Lithium Tantalate composite embedded with Silver nano-particles	PVT:LT-Ag	Thick-Films	f(T)	f(T)	Present work
8	Modified Lead Metaniobate	PN	Bulk Ceramic	f(T)	f(T)	Present work
9	Modified Lead Titanate	MPT	Bulk Ceramic	f(T)	f(T)	Present work
10	Cement – nanoCarbon Fiber Composite (0.63% nanoCarbon fibers)	Ce-NFC	Bulk Ceramic	f(T)	f(T)	Present work

f(T)* - parameter (p; ε') function of temperature.
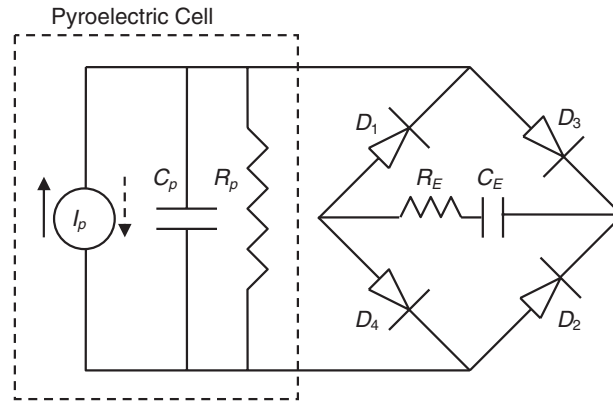
Fig. 1 Pyroelectric cell with full bridge rectifier circuit for charge storage; D_1–D_2 are used in one direction of current flow (solid arrow), D_3–D_4 are used when current flows in the opposite direction.

Lithium tantalate ($LiTaO_3$; LT) with perovskite structure is widely applied in pyroelectric point detectors due to its high pyroelectric coefficient and low relative dielectric constant.[20] It has excellent mechanical stability, making it a good candidate for piezoelectric materials as well.

b. Polycrystalline pyroelectric materials: A wide range of polycrystalline materials with perovskite structure is available for pyroelectric device applications, such as PZT, PLZT, multilayered PZT films, and others.[20] These ceramics are relatively low in cost to manufacture by using standard mixed-ceramic oxide processing steps, and are both mechanically and chemically robust. These properties seem suitable for use in the proposed application: energy harvesting by embedding in roads.

c. Composite pyroelectric materials: There are also organic ferroelectric as well as pyroelectric materials available, such as, Poly vinylidene fluoride ($(CH_2$-$CF_2)n$; PVDF) and its co-polymer with trifluoroethylene P(VDF-TrFE) (70/30). PVDF and P(VDF-TrFE) copolymer consists of a crystalline and an amorphous fraction. Unlike PVDF, the introduction of a small amount of TrFE causes the copolymer to crystallize directly into the β phase from the melt. The P(VDF-TrFE) copolymer is therefore made to be pyroelectric without stretching, as with PVDF. In the $-40°C$ to $+100°C$ temperature ranges, both show significant pyroelectric and piezoelectric behavior.[20] Thus, it is worth investigating polymer composites: silver nanoparticles embedded in P(VDF-TrFE):LT (PVT:LT-Ag) and Portland cement-nanocarbon fiber reinforced (Ce-NFC) composites. Thus, these were fabricated in bulk and thick film forms,[26] respectively. To prepare the cement composite specimens, the ordinary Portland cement, poly-vinyl alcohol (PVA), and carbon nanofibers were mixed thoroughly. PVA acts as a binder within the cement. No aggregate was added. The carbon nano-fiber (PR-19-XT-LHT) was obtained from Pyrograph Products, Inc. Cedarville, Ohio. The weighed mixture of cement composite was mixed in water to make a paste of suitable viscosity. The paste was compressed in a steel mound to form disks of diameter 10 mm and thickness 2.0 mm approximately. The disks were then cured at 25°C at 100% humidity for 24 h to speed up the hydration process of the cement matrix. The preparation technologies of the composites and the above cited materials have been recently presented by Batra et al. elsewhere.[18,20]

2.2 Pyroelectric Coefficient (p) and Dielectric Constant (ε')

The relevant parameters required for energy harvesting modeling including the dielectric constant (ε') and pyroelectric coefficient (p) of selected materials were calculated or obtained from
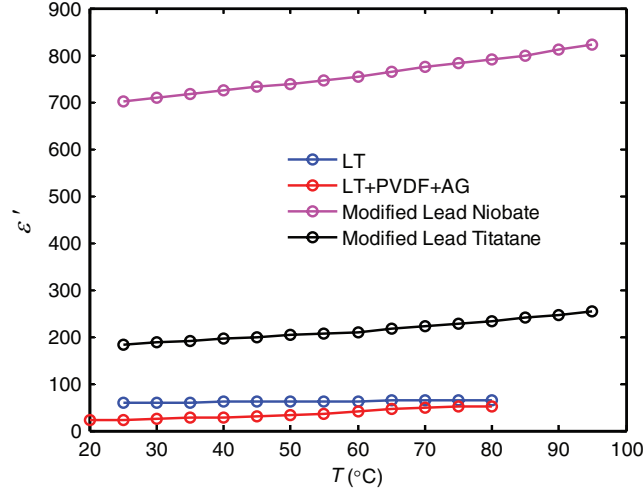
Fig. 2 The variation of dielectric constant (ε') with the temperature of a few selected pyroelectric materials.

the literature. A real part (ε') of the dielectric constant were determined as:

$$\varepsilon' = \frac{C_P d}{\varepsilon_0 A},$$ (1)

where C_p is the parallel capacitance of the sample at signal frequency of 1 kHz, A is the electrode area (identical areas for the opposite electrodes were used in each sample), d is the thickness of the sample, and $\varepsilon_0 = 8.854 \times 10^{-12}$ F/m is the permittivity of vacuum. To record the dynamic relative pyroelectric current I_p, the direct method of Byer and Roundy was used.[17]

The pyroelectric current I_p was measured at various temperatures at a constant heating rate, and the pyroelectric coefficient (p) was calculated using the relationship:

$$p = \left(\frac{I_P}{A}\right) \bigg/ \left(\frac{dT}{dt}\right),$$ (2)

where dT/dt is the rate of change of temperature, which was kept constant throughout the measurement. The change in pyroelectric coefficient indicates the change in dipole orientation inside the material; the higher the coefficient, the better the material is for converting temperature change in electrical charge. The additional charge generated via heating or cooling within a temperature change, dT, can be calculated as:

$$dQ = dI_P dt = pA\frac{dT}{dt}dt = pAdT.$$ (3)

The detailed measurement procedures of the parameters such as capacitance (C_p) and pyroelectric current (I_p; p) are used for simulation are described by Batra et al. in earlier publications.[17,18]

3 Results and Discussion

3.1 Electrical Parameters

Figures 2 and 3 show the dependence of dielectric constant (ε') and pyroelectric coefficient (p) on temperature of selected materials listed in Table 1. All of the materials show the dependence of ε' and p over temperature; ε' and p increase with an increase in temperature as expected in pyroelectrics. Modified lead niobate shows the highest ε' whereas PVT:LT-Ag
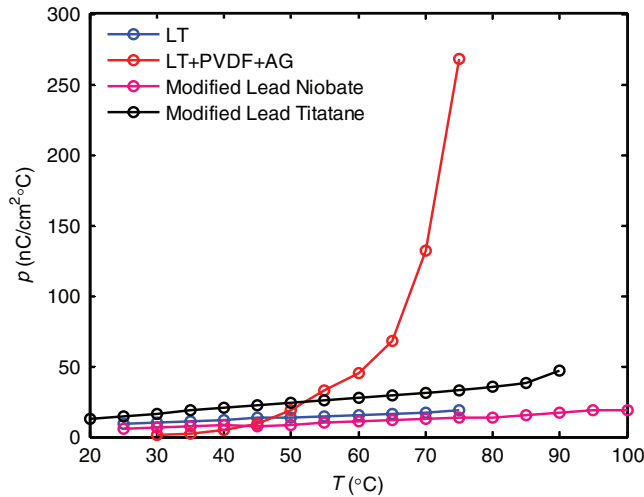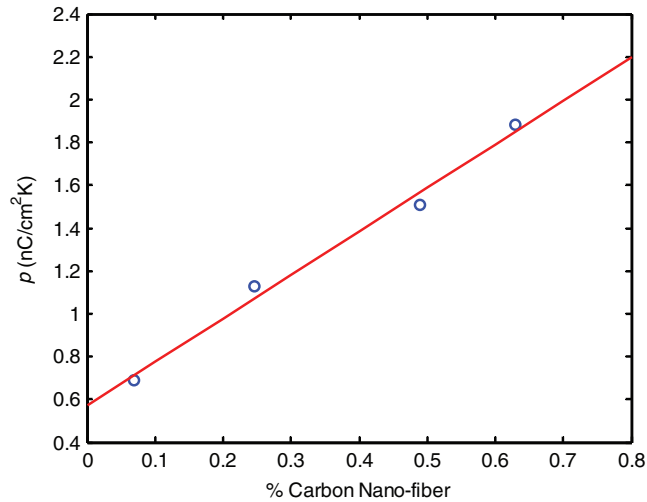
Fig. 3 The variation of pyroelectric coefficient (p) with the temperature of a few materials investigated.

shows the lowest. The highest pyroelectric coefficient is obtained from PVT:LT-Ag composite. In the case of the cement composites, p also increases with the increase in carbon nanofiber content (Fig. 5). The observed increase in p of cement composite with carbon nanofiber with the increase in temperature is different from that reported by Wen and Chung.[25] Figure 4 shows the variation of ε' for the cement composite with different percentages of carbon nanofiber content. The observed increase in dielectric constant in cement composites can be attributed to the increase in mobility of ions as the temperature increases, whereas in the case of other materials, the increase of ε' is due to the increase in dipolar moments in the material. It is evident that ordinary Portland cement behaves similar to typical pyroelectric materials.
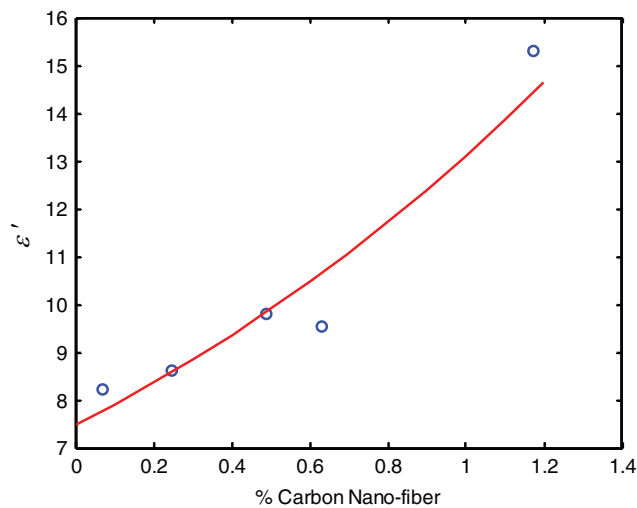

Fig. 4 The variation of dielectric constant (ε') of Ce-NFC composite with percent of nanocarbon fibers' content (at 1 kHz and 40°C).

Fig. 5 The variation of pyroelectric coefficient (p) of Ce-NFC composite with the percent of nanocarbon fibers' content (at 1 kHz and 40°C).

3.2 Energy Harvesting Capacity of Materials Investigated Through Modeling and Numerical Simulation

The pyroelectric electric generator is modeled as a current source with a capacitor and a resistor in parallel with a current source.[20] The current is generated within the cell with the change in temperature. Figure 1 shows the circuit used to model pyroelectric sensors used for energy conversion and charge storage. Equation (2) indicates that the pyroelectric current is directly proportional to the rate of change of temperature. However, one problem with this behavior is that the current will flow in the opposite direction when the rate changes from positive to negative or from negative to positive. In other words, heating followed by cooling or cooling followed by heating will produce charge accumulation in a different direction. However, to charge an external capacitor it is essential that the capacitor be charged continuously. To mitigate the problem, a full bridge diode rectifier circuit, as shown in Fig. 1, can be used. The pyroelectric source is connected to an external capacitor (C_E) and an external resistor (R_E). There are two
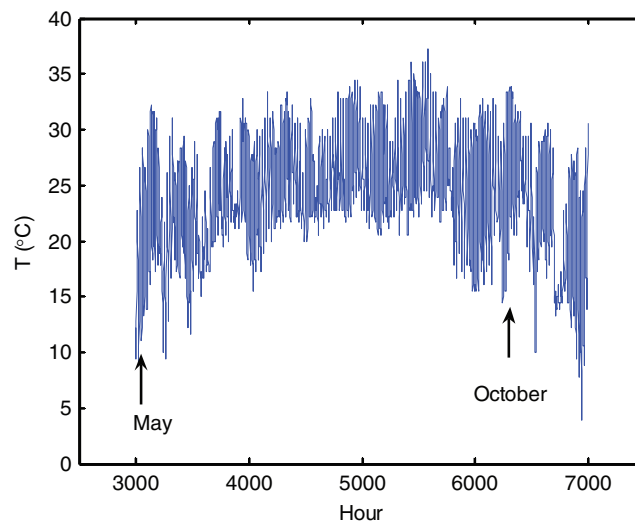
Fig. 6 Temperature profile (May to October) at Huntsville, Alabama (USA); (Station ID 03856).
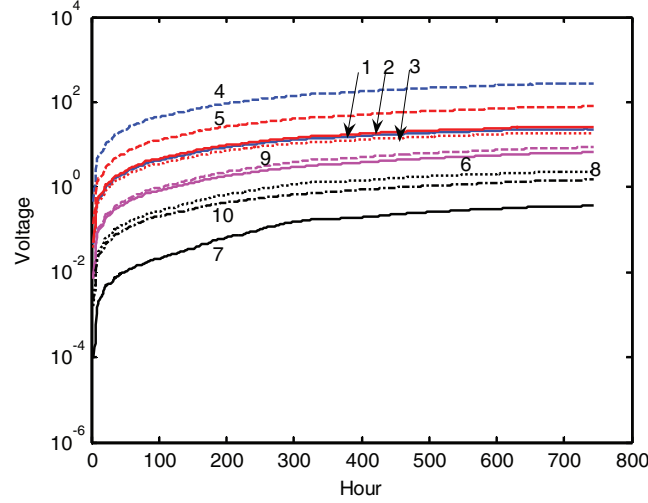
Fig. 7 The voltage generated via storing charges in a capacitor due to typical variation of temperature during the month of May (as per Fig. 6); legends: 1—DPZT, 2—PLZT, 3—PZTML, 4—TGSe, 5—PLZT-1, 6—LT, 7—PVT:LT-Ag, 8—PN, 9—MPT, 10—Ce-NFC.

pairs of diodes; one pair is used for each direction of charge flow. Diodes (D_1–D_2) are used when charge is flowing in one direction and diodes (D_3–D_4) are used when the charges flow in the other direction. At each time only the forward biased diodes work, the other two pairs block the current flow under reverse biased condition. As it can be seen, in both cases the external capacitor (C_E) is charged via charge flows in one direction and that causes the voltage to increase across the external storage capacitor.

The charge flow in the two-capacitor system can be modeled as follows: When the new charge is accumulated, it is distributed in both capacitors and the charge balance equation can be written as:[14]

$$\Delta Q_n = Q_{E,n} - Q_{E,n-1} + Q_{P,n} \pm Q_{P,n-1}, \tag{4}$$

$$
\begin{aligned}
Q_{P,n} &= V_n C_P, \\
Q_{P,n-1} &= V_{n-1} C_P, \\
Q_{E,n} &= V_n C_E, \\
Q_{E,n-1} &= V_{n-1} C_E,
\end{aligned}
\tag{5}
$$

where C_p and C_E are pyroelectric cell capacitance and external charging capacitance, respectively, V_n and V_{n-1} are voltage at temperature data points n and $n-1$, respectively, Q_p and Q_E are charge accumulated in the pyroelectric cell and the external capacitance, respectively, and ΔQ_n is the additional charge generated at the n'th data point (from heating or cooling). The $\pm$ sign in front of the right-hand side term indicates that current generated in the pyroelectric cell can be in the opposite direction if the sign of the rate of change of temperature changes from $(n-1)$'th datum point to n'th datum point.

The substitution of Eq. (5) into Eq. (4) results in the following recurrence equation, from which the voltage across the external capacitance can be calculated at a given temperature datum point:

$$V_n = \frac{\Delta Q}{C_P + C_E} + \left(\frac{C_E \pm C_P}{C_E + C_P}\right) V_{n-1} = \frac{p A \Delta T}{C_P + C_E} + \left(\frac{C_E \pm C_P}{C_E + C_P}\right) V_{n-1}. \tag{6}$$
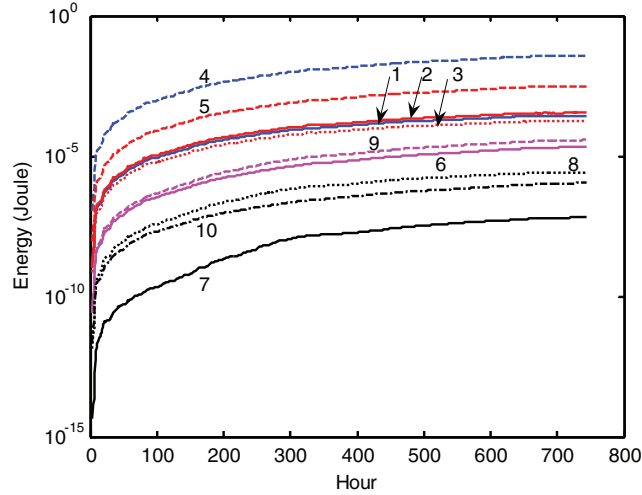
Fig. 8 The electric energy generated via storing charges in a capacitor due to typical variation of temperature during the month of May (as per Fig. 6); legends: 1—DPZT, 2—PLZT, 3—PZTML 4—TGSe, 5—PLZT-1, 6—LT, 7—PVT:LT-Ag, 8—PN, 9—MPT, 10—Ce-NFC.

Once the voltage is determined, the energy stored at n'th datum point can be calculated from the following equation:

$$E_n = 0.5 C_E V_n^2. \tag{7}$$

Equations (6) and (7) have been used to simulate the voltage and energy produced, respectively, from a measured temperature profile of actual pavement temperature. Figure 6 shows the temperature profile between May to October at a weather station location in Huntsville, Alabama. The temperature profile was obtained from the Environmental and Climatic Database of Mechanistic Empirical Pavement Design Guide (MEPDG).[27]

When storing energy from temperature change/fluctuations, the values of C_P and C_E should be optimized for the highest energy storage. Furthermore, the external resistor, R_E, and the external capacitor, C_E, can be adjusted to obtain fast charging. The parameters of the materials presented in Table 1 have been used for the simulation. The simulated voltage and energy stored are shown in Figs. 7 and 8 for the materials shown in Table 1, respectively. The circuit is simulated assuming 1 cm^2 area of the pyroelectric cell with 0.1-cm thickness. The external storage capacitor is assumed to be 1.0 μF. For the materials for which the pyroelectric coefficient and the dielectric constant are functions of temperature, the actual functional relationship has been used; for other materials, constant values of p and ε' have been used. The capacitance of the pyroelectric element was determined using Eq. (1). Figure 7 shows the accumulated voltage for 800 h during the month of May starting from zero voltage. Figure 8 shows the associated accumulated energy (in Joules). The highest maximum voltage accumulated during the month of May is approximately 278 V from TGSe and the corresponding electric energy is approximately 0.04 J. It is worth mentioning that this maximum voltage can be controlled by choosing a suitable value for external storage capacitor, C_E; however, for the present modeling and numerical simulation of value of the electric energy in Huntsville, Alabama, the capacitance of 1.0 μF is utilized.

4 Conclusion

In this study, important pyroelectrics in single- and polycrystalline and nanocomposite forms have been fabricated and/or obtained. The dielectric and pyroelectric properties of some of the materials fabricated have been determined. The materials' parameters of interest have been

used to perform numerical simulation with actual pavement temperature data obtained from the climatic database of MEPDG.[27] The numerical simulation performed indicates that the methodology and model adopted are sound. Among the pyroelectrics selected for simulation, TGSe is an attractive candidate for energy harvesting from pavements due to its higher pyroelectric coefficient near ambient temperatures. Pyroelectric current (energy) is typically a function of dT (change in temperature) at a given temperature; for larger temperature (T), the energy generated will be high; higher values of both *p* and dT will give higher energy generated.

Its real application will determine if the predicted performance can be realized or not. To fabricate and embed an EH module based on TGSe materials, a technology has to be developed.

It is worth mentioning that electric energy generated due to pyroelectricity in the pavement is location, traffic, time, and population specific due to temperature variation of the pavement in consideration. Since ambient temperature variations, and hence pyroelectric current, in pavement depend on location; for optimum performance, the suitable pyroelectric material-based energy harvesters including the electric circuit have to be selected and designed accordingly. However, only the field applications of pyroelectric materials investigated will determine the suitability of the material based on life, weathering, cost-analysis, and ease of embedding in pavements.

It will be also interesting and important to investigate electric energy generated via both pyroelectric and piezoelectric properties of the same selected material. The hybrid and multi-module energy harvesters can then be designed and fabricated by connecting these elements in a suitable electric circuit. Thus, enhancement of charge-storage rate in the capacitor will be possible.

Further work is in progress to investigate their performance, suitability, and economics by embedding single-element energy harvesters in pavements under laboratory simulated conditions.

Acknowledgments

References

1. S. Priya and D. J. Inman, Eds., *Energy Harvesting Technologies*, Springer, New York (2009).
2. S. Roundy, P. K. White, and J. Rabaey, *Energy Scavenging for Wireless Sensor Networks with Special Focus on Vibration*, Kluwer Academic Publishers, Boston, Massachusetts (2004).
3. S. Beeby and N. White, *Energy Harvesting for Autonomous Systems*, Artech House, Norwood, Massachusetts (2010).
4. Web Access: http://www.pavegensystems.com/, accessed July 29, 2010.
5. Web Access: http://www.innowattech.co.il/, accessed July 29, 2010.
6. A. K. Batra, M. D. Aggarwal, P. Guggilla, M. E. Edwards, P. G. Penn, and J. R. Currie Jr., "Pyroelectric materials for uncooled infrared detectors: processing, properties and applications," *NASA Tech. Memo.* **NASA/TM-2010-6373**, 1–71 (2010).
7. M. T. Penella and M. Gasulla, "A review of commercial energy harvesters for autonomous sensors," in *Proceedings of the Inst. Meas. Tech. Conference – IMTC 2007* (2007).
8. S. P. Beeby, M. J. Tudor, and N. M. White, "Energy harvesting vibration sources for microsystems applications," *Meas. Sci. Technol.* **17**, R175–R195 (2006).

9. N. Shenck and J. Paradiso, "Energy scavenging with shoe-mounted piezoelectrics," *IEEE MICRO* **21**(3), 30–42 (2001).

10. H.-U. Kim, W.-H. Lee, H. V. Rasika Dias, and S. Priya, "Piezoelectric microgenerator-current status and challenges," *IEEE Trans. Ultrason. Ferroelectr. Freq. Control* **56**(8), 1555–1568 (2009).

11. G. Sebald, E. Lefeuvre, and D. Guyomar, "Pyroelectric energy conversion: Optimization principles," *IEEE Trans. Ultrason. Ferroelectr. Freq. Control* **55**, 538–551 (2008).

12. S. Bauer, "Piezo-, pyro- and ferro-electrets: Soft transducer materials for electromechanical energy conversion," *IEEE Trans. Dielectr. Electr. Insul.* **13**(5), 953–962 (2006).

13. R. C. Buchanan and J. Huang, "Pyroelectric and sensor properties of ferroelectric thin films for energy conversion," *J. Eur. Ceram. Soc.* **19**, 1467–1471 (1999).

14. A. Cuadrasa, M. Gasulla, and V. Ferrari, "Thermal energy harvesting through pyroelectricity," *Sens. Actuators, A* **158**, 132–139 (2010).

15. J. Xie, X. P. Mane, C. W. Green, K. M. Mossi, and K. Leang, "Performance of piezoelectric materials for pyroelectric energy harvesting," *J. Intell. Mat. Syst. Struct.* **21**, 243–249 (2009).

16. A. K. Batra, M. D. Aggarwal, and R. B. Lal, "Growth and characteristics of TGS crystals grown in microgravity environment of space and on earth: An update," in *Crystal Growth of Technologically Important Materials*, Allied Publishers Pvt. Ltd., New Delhi, India (2003).

17. A. K. Batra, J. R. Currie, S. K. Aggarwal, M. D. Aggarwal, and R. B. Lal, "Present status of TGS-based pyroelectric infrared detectors and computational simulation of their integration with silicon technology," *Proc. SPIE* **5209**, 133–147 (2004).

18. A. K. Batra, M. D. Aggarwal, M. Edwards, and A. S. Bhalla, "Present status of polymer: Ceramic composites for pyroelectric infrared detectors," *Ferroelectrics* **366**, 84–121 (2008).

19. M. D. Aggarwal, A. K. Batra, R. B. Lal, B. G. Penn, and D. Frazier, "Growth and characteristics of bulk crystal grown from solution on earth and microgravity," in *Handbook of Crystal Growth*, Springer, New York (2010).

20. A. K. Batra, M. D. Aggarwal, P. Guggilla, M. E. Edwards, P. G. Penn, and J. R. Currie, Jr., "Pyroelectric materials for uncooled infrared detectors: Processing, properties and applications," *NASA Tech. Memo* **NASA/TM-2010-6373**, 1–71 (2010).

21. A. Khodayari, S. Pruvost, G. Sebald, D. Guyomar, and S. Mohammadi, "Nonlinear pyroelectric energy harvesting from relaxor single crystals," *IEEE Trans. Ultrason. Ferroelectr. Freq. Control* **56**, 693–699 (2009).

22. H. Zhu, S. Pruvost, D. Guyomar, and A. Khodayari, "Thermal energy harvesting from $Pb(Zn_{1/3}Nb_{2/3})_{0.955}Ti_{0.045}O_3$ single crystals phase transitions," *J. Appl. Phys.* **106**, 124102 (2009).

23. A. Navid, C. S. Lynch, and L. Pilon, "Purified and porous poly(vinylidene fluoride-trifluoroethylene) thin films for pyroelectric infrared sensing and energy harvesting," *Smart. Mater. Struct.* **19**, 055006 (2010).

24. P. Guggilla, A. K. Batra, and M. E. Edwards, "Electrical characterization of $LiTaO_3$:P(VDF-TrFE) Composites," *J. Mater. Sci.* **44**, 5469–5479 (2009).

25. S. Wen and D. D. L. Chung, "Pyroelectric behavior of cement-based materials," *Cem. Concr. Res.* **33**, 1675–1679 (2003).

26. A. K. Batra, J. Corda, P. Guggilla, M. D. Aggarwal, and M. E. Edwards, "Electrical properties of silver nanoparticles reinforced $LiTaO_3$:P(VDF-TrFE) composite films," *Proc. SPIE* **7419**, 741904 (2009).

27. *Guide for Mechanistic Empirical Design of New and Rehabilitated Pavement Structures: Final Report*, National Cooperative Highway Research Program (NCHRP) (2004). NCHRP Project No. 1-37A, Transportation Research Board, National Research Council, Washington DC.

Biographies and photographs of the authors not available.